Kinetic Pathway for the Formation of Fe Nanowires on Stepped Cu(111) Surfaces

Yina Mo,[1] Kalman Varga,[2,4] Efthimios Kaxiras,[1,3] and Zhenyu Zhang[4,2]
[1]*Physics Department, Harvard University, Cambridge, Massachusetts 02138, USA*
[2]*Department of Physics, University of Tennessee, Knoxville, Tennessee 37996-1200, USA*
[3]*Division of Engineering and Applied Sciences, Harvard University, Cambridge, Massachusetts 02138, USA*
[4]*Oak Ridge National Lab, Condensed Matter Science Division, Oak Ridge, Tennessee 37831, USA*
(Received 3 November 2004; published 22 April 2005)

We report the discovery of a novel kinetic pathway for the formation of one-dimensional Fe nanowires of single atom width on stepped Cu(111) surfaces. This pathway, identified through extensive total-energy calculations within density functional theory, establishes that the stable structure involves a row of Fe atoms on the *upper* edge of a step. The formation of the surface wire is preceded by facile incorporation of an initial row of Fe atoms into the surface layer at one lateral lattice constant away from the step edge, which then acts as an attractor for the second exposed row of atoms. The resulting wire structure provides a natural interpretation of existing experimental results. We also explore the applicability of this mechanism in the formation of other related systems.

DOI: 10.1103/PhysRevLett.94.155503 PACS numbers: 81.07.Vb, 61.46.+w

One-dimensional (1D) electron systems are expected to possess many unconventional physical properties, most notably non-Fermi liquid behavior [1]. Unambiguous confirmation of such properties has been sparse, largely because of the difficulty in obtaining truly 1D electron systems [2,3]. Among various approaches to overcome the formation bottleneck, growth of quantum wires through decoration of surface steps has received intensive attention [4]. Example systems include metallic wires on semiconducting [5,6] or insulating substrates [7] and magnetic wires on nonmagnetic metal substrates [8–12]. The former class of quantum wires serves as testing ground for electrical transport in quasi-1D systems; the latter offers opportunities to study magnetism and spin transport in 1D systems.

In recent experimental studies of magnetic wires on stepped metal surfaces, most of the wires were found to form at the lower edge of monatomic-layer-high steps [10–12]. This prevailing feature is not too surprising, because an adatom of a given magnetic element typically prefers to occupy a stable adsorption site located at the lower edge of a step, thereby leading to the nucleation and growth of a wire along the lower step edge. In light of this general trend, the experimental observation that Fe wires of varying widths are formed at the *upper* step edges on a vicinal Cu(111) surface [8] was rather surprising. Because of the intriguing magnetic properties of these Fe wires, the initial observation stimulated an extensive line of experimental and theoretical studies aimed at explaining the microscopic origin of the magnetic properties [13–15]. In essentially all these previous studies, the magnetic properties were explored for given static Fe wire structures. It remains a mystery why such Fe wires prefer to form at the upper edges of steps, and what the kinetic mechanisms are that lead to their formation.

In this Letter, we resolve this long-standing puzzle by revealing the kinetic mechanism involved in the formation of Fe wires at the upper edges of steps on the Cu(111) surface. Using extensive total-energy calculations within density functional theory (DFT), we find that an Fe wire at the upper edge, with an *apparent* width (as likely to be detected by a scanning tunneling microscope) as narrow as one atom, is already energetically more stable than the corresponding structure at the lower edge of the step, but only under the condition that another row of Fe atoms be incorporated underneath the exposed row. The kinetic pathway for the formation of such a novel wire structure involves two phases. First, a row of Fe atoms are incorporated into the upper terrace, one lateral lattice constant away from the step edge. This is the energetically preferred and kinetically accessible final configuration whether the Fe adatoms approach the step from the upper or from the lower terrace. Subsequently, additional Fe adatoms diffusing on the terrace are strongly attracted to the buried basal wire, thereby forming an atomic wire exposed at the upper edge. We discuss this central finding in comparison with existing experiments. We also attempt to rationalize the preference of the two-phase kinetic pathway based on generic qualitative arguments, and support these arguments by examining related systems.

The DFT results reported here are obtained with the VASP code [16], using the Perdew-Wang 1991 version of the generalized gradient approximation (PW91-GGA) [17]. The default plane-wave cutoffs for different elements from the GGA ultrasoft-pseudopotential database [18] are adopted in the calculations. The Fermi-level smearing approach of Methfessel and Paxton [19] is employed for the electronic states near the Fermi level, with a Gaussian width of 0.2 eV. Optimized atomic geometries are achieved when the forces on all the unconstrained atoms are smaller in magnitude than 0.01 eV/Å. The bulk Cu lattice constant determined with these computational parameters is 3.645 Å, which compares well with the experimental value of 3.63 Å. The climbing image nudged elastic band (NEB) method is applied to locate the transition state, and typically four slab replicas between the initial and final states are sufficient to produce a smooth minimum energy path [20]. We also use a spline interpolation fit to examine the stability of the NEB calculations and determine the potential energy barriers more accurately.

There are two types of steps on Cu(111), referred to as A and B, with the former having lower formation energy [21]. Experimentally, Fe wires have been observed to form on the upper edges of both types of steps [22]. Hence, in the present study we focus our attention on growth of Fe wires on A-type steps. Following Ref. [23], we model the stepped Cu surface by a slab miscut along the (322) direction, consisting of (111) terraces of width five lateral lattice constants separated by type A steps of monatomic height. The slab used in the calculations contains six layers and a total of 96 Cu atoms in the periodic supercell. The bottom three layers are fixed at their respective bulk positions during the relaxation (calculations using a nine-layer slab produce similar energy difference of selective configurations). A $2 \times 2 \times 1$ mesh in the Brillouin Zone of the supercell is used to sample the reciprocal space. As convergence checks, calculations of several important energy differences and activation barriers using a $3 \times 3 \times 1$ mesh lead to insignificant variations to the values from the use of a $2 \times 2 \times 1$ mesh. The vacuum region separating slabs is equivalent to 11.5 Å.

We first study the interaction of a single Fe adatom with the stepped surface. Our calculations show that the preferred adsorption site of an Fe adatom is always the fcc site, whether it is in the central region of a terrace or in the immediate vicinity of the step. In contrast, the activation energy barrier encountered by the adatom when it moves on the surface can differ significantly in the two regions. For terrace diffusion, the preferred mechanism is via direct hopping, with an activation energy barrier of 0.025 eV. When reaching a step from the upper edge [Fig. 1(a)], an Fe adatom would have to overcome a barrier of 1.00 eV if it were to climb down by direct hopping over the step edge (Fig. 1, $A_1 \rightarrow B_1$). A naïve interpretation of this result suggests that the high energy barrier for downward motion of Fe adatoms over the step edge would offer an explanation for the formation of Fe wires at the upper step edges of the Cu(111) surface. But the real physical situation is more intricate, and thereby more challenging. The Fe adatom, instead of hopping down against the high energy barrier, can easily be embedded into the Cu layer through an exchange process (Fig. 1, $A_1 \rightarrow D_1$) with an energy barrier of only 0.07 eV. Furthermore, the Cu atom displaced by the Fe adatom in the exchange process prefers to stay at the lower edge of the step, adjacent to the embedded Fe atom, because it would have to overcome a high activation barrier of about 0.9 eV in order to reach the nearest hcp site away from the step edge.

The above discussion establishes how an Fe adatom approaching the step from the upper terrace will end up embedded in the step edge. Fe adatoms can also approach a step from the lower terrace. It is therefore necessary to examine the optimal final configuration for this situation. Here, we find that the Fe atom switches position with a Cu atom at the step edge through a slightly more complex motion involving an intermediate state C_1. The Fe atom is first incorporated into the step by displacing a Cu atom upward onto an hcp site at the upper step edge [Fig. 1(c)], a process which has an activation barrier of 0.66 eV (Fig. 1, $B_1 \rightarrow C_1$); subsequently, the displaced Cu atom hops off the step directly to the lower terrace, a process with an activation barrier of 0.34 eV (Fig. 1, $C_1 \rightarrow D_1$); we refer to this motion as the "assisted exchange" process. Thus, independent of the direction in which the Fe adatom approaches the step edge, there is a unique stable final configuration, shown in Fig. 1(d).

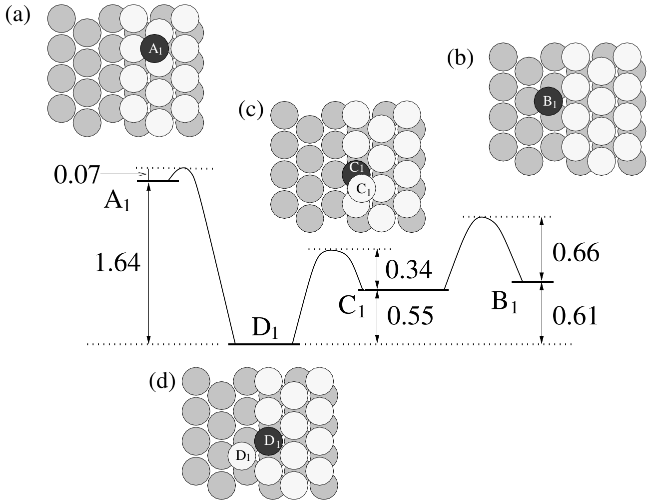

FIG. 1. Top view of the surface model employed in the calculations, showing the first phase of Fe wire formation. The white and gray circles represent Cu atoms in the first and second layers, respectively; the black circles represent Fe atoms. (a) Initial configuration of an Fe adatom reaching the step from the upper terrace. (b) Initial configuration of an Fe adatom reaching the step from the lower terrace. (c) Intermediate state of the Cu-Fe assisted exchange as the state B_1 converts to the final state D_1 in (d), which is also the stable final configuration from A_1 after place exchange. The relative energies and the activation barriers (in eV) connecting the different configurations are indicated next to vertical arrows.

When a second Fe adatom approaches the step containing an embedded Fe atom from the upper edge, it is even more preferred to join the first one and extend the embedded wire to two atoms in length, gaining an energy as much as 2.52 eV. Additional Fe atoms approaching the step edge will undergo the same processes, leading to a row of Fe atoms embedded in the Cu step, one lateral lattice constant away from the step edge. This embedded row of Fe atoms has so far escaped experimental detection. However, our study shows that it is an essential part of wire growth.

We next consider the deposition of additional Fe atoms on the surface containing mixed Fe-Cu steps. The likely configurations are shown in Fig. 2. Again, an Fe adatom can approach the mixed step from either the upper or lower terrace. From the upper terrace, configuration A_2 is easily reached, which is energetically stable because of the attraction of the Fe adatom to the basal Fe wire. In contrast, configuration B_2, reached by an Fe adatom approaching from the lower terrace, is energetically very unstable. In analogy to the processes shown in Fig. 1, the high energy configuration B_2 will convert into A_2 via two intermediate states C_2 and D_2. Configuration C_2 is reached via a place exchange process, with the Fe adatom taking the place of an edge Cu atom, and the Cu atom displaced up to reside on top of three Fe atoms. Configuration D_2 is reached when the atop Cu atom climbs down the Fe-Cu mixed step. Finally, the $D_2 \rightarrow A_2$ transition is realized via a second assisted process. Based on the relative energies shown in Fig. 2, and the detailed calculations for the first phase (Fig. 1), we surmise that the kinetic barriers encountered in the overall $B_2 \rightarrow A_2$ transition are all relatively small (up to a few tenths of eV). Therefore, additional deposition of Fe on the surface naturally leads to the growth of an Fe wire on top of the Fe basal wire, with an *apparent* width of only one atom. Further growth of Fe will widen the width of the wire, but the narrowest stable Fe wire is a true one-atom-wide structure residing at the upper edge of the mixed Fe-Cu step.

So far we have identified a two-phase kinetic pathway for the formation of an Fe wire at the upper edge of a step on a Cu(111) surface. Next, we attempt to rationalize the preference of the two-phase kinetic pathway for this system based on qualitative considerations of bond strength, bond length, and crystalline structure.

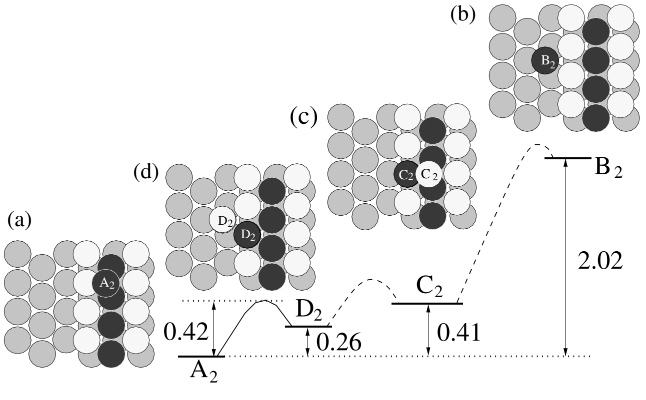

FIG. 2. Top view of the second phase of the two-phase kinetic pathway for Fe wire formation on the stepped Cu(111) surface, together with the energy levels and activation barriers (in eV) for different configurations. Dashed lines indicate energies not explicitly calculated. (a) and (b) show the initial configurations reached when an Fe adatom approaches the Fe-Cu mixed step from the upper and lower terrace, respectively. Configuration A_2 is energetically most stable, because of the strong attraction by the buried Fe wire. Configuration B_2 is energetically very unstable, and will convert to configuration A_2 via two intermediate configurations shown in (c) and (d).

First, the preference of the various motions shown in Figs. 1 and 2 is tied to the inequality chain in the Fe-Fe, Fe-Cu, and Cu-Cu bond strengths: $U_{\text{Cu-Cu}} < U_{\text{Cu-Fe}} < U_{\text{Fe-Fe}}$, deduced from the melting temperatures $T_m(\text{Fe}) = 1811\text{K} \gg T_m(\text{Cu}) = 1358$ K. Compared with direct hopping, the exchange processes have lower activation energies because they involve interruption of fewer of the stronger Cu-Fe or Fe-Fe bonds [24].

On the other hand, consideration of pure bond strength alone is insufficient in explaining the structural selection in phase two. Here, both the bond length and the intrinsic crystal structure come into play. This is because of the different nature of the configurations involved in the two phases: the first phase involves Fe *adatoms* on a Cu substrate, dealing with the behavior of individual Fe atoms with a surrounding Cu host. The second phase, with the involvement of the Fe atoms *embedded* in the Cu substrate, deals with Fe atoms in an environment more akin to the crystal structure of bulk Fe. In the $\langle 011 \rangle$ direction of the Cu(111) surface, the nearest Cu-Cu distance is 2.56 Å, while in bcc Fe the nearest Fe-Fe distance in the $\langle 111 \rangle$ direction is 2.48 Å. Therefore, the embedded Fe row is only minimally strained by the fcc structure of the Cu substrate. In order for the Fe atoms to regain an environment closer to their preferred bcc crystalline structure, incoming Fe atoms in phase two choose to stay on the upper edge of the step. This avoids undergoing either more embedding of the Fe atoms, which would lead to an extended Fe structure in fcc geometry, or direct hoppings, which would not promote growth of a bcc-like Fe crystal.

To explore the applicability of this two-phase kinetic process to other systems, and, in particular, to justify the physical considerations involved in the second phase of the wire formation, we next examine the behavior of Co and W atoms on the same stepped Cu(111) surface.

Because Fe, Co, and W have the same bond strength inequalities when growing on Cu, we expect that the exchange pathways similar to those shown in Fig. 1 should also take place for Co or W, leading to the formation of a row of atoms embedded into the Cu substrate, one lateral lattice constant away from the step edge (phase one). But different expectations from the Fe case arise in phase two. The Co crystal has a hexagonal structure. Its densely packed (0001) surface has exactly the same hexagonal configuration as the (111) surface layer of the Cu substrate. The Co nearest neighbor distance on the (0001) surface is 2.51 Å, which enables the buried Co line to be accommodated at the regular lattice sites of the fcc Cu substrate even better than Fe. Furthermore, additional Co atoms should also be embedded into the Cu substrate as an extension of the Co structure in the hexagonal geometry, thereby doubling the width of the buried Co wire. W, like Fe, prefers a bcc structure, but its nearest neighbor distance in the $\langle 111 \rangle$ direction is 2.74 Å, much larger than the corresponding distance of 2.56 Å for Cu. Therefore, when a row of W atoms are embedded into the Cu substrate, we expect the relaxation of the ensuing strain to lead to buckling of the W

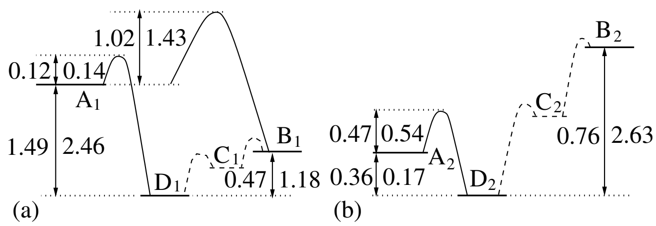

FIG. 3. Relative energies and activation energy barriers (in eV) of configurations involved in (a) phase one and (b) phase two of the kinetic pathway for Co (numbers to the left of vertical arrows) and W (numbers to the right). Dashed lines indicate energies not explicitly calculated.

row, which would then spoil its alignment with the ⟨111⟩ direction. Additional incoming W atoms should follow the structure of this buckled basal line.

As shown in Fig. 3, our detailed calculations confirm these qualitative expectations. In the first phase, when approaching the step from the upper edge as shown in Fig. 1(a), both the Co and the W adatom will undergo the exchange pathway to reach the final state D_1. For the initial configuration B_1, which involves a Co or W adatom approaching from the lower terrace, the final state D_1 has a much lower energy (0.47 eV for Co and 1.18 eV for W), ensuring that it is the final stable configuration that can be reached via (assisted) exchange. However, the presence of a basal line in the Cu substrate does not guarantee the formation of a stable wire on top. A detailed examination shows that the embedded Co row is nicely confined in the substrate while the W row buckles to partially recover the bcc structure in the ⟨011⟩ direction. When additional Co or W adatoms approach the mixed step from the upper edge, they continue to embed into the step via place exchanges. Such processes favor the stabilization of the hexagonal structure of Co or the bcc structure of W. Based on these results, we conclude that the same type of wire as for the Fe case is unlikely to form for either Co or W. Instead, a Co atom wire, sitting on top of two buried rows of Co, is favored, while the case of W is more complex because of buckling.

Finally, note that we have also carried out spin-polarized calculations with all-electron methods [25]. These results do not alter the central conclusions of the spin-averaged calculations. Spin-polarized calculations may slightly change the detailed configurations of the top wire, but for the kinetic processes and the 1D wires we have focused on, our original calculations give reliable conclusions. Therefore, we expect that growth experiments with carefully controlled Fe coverages should observe the initial burying of the Fe rows and the subsequent formation of Fe wires of single atom width. Furthermore, our findings suggest the need for a reexamination of conclusions from previous studies of the magnetic properties of Fe wires that have overlooked the necessary existence of the Fe basal line.

In conclusion, our extensive theoretical study of the kinetics of Fe adatoms on the Cu(111) stepped surfaces provides the missing kinetic picture of how Fe nanowires are formed. A hidden Fe basal line under the exposed wire has been identified. The underlying physical reasons for the kinetic pathway are also corroborated by the results of additional calculations for Co and W.

We thank Dr. Wenguang Zhu and Dr. Yu Jia for technical help, and Dr. Jian Shen for helpful discussions related to the experiments. This work was partly supported by NSF (Institute for Theory of Advanced Materials in Information Technology, Grant No. DMR-0325218, and Grant No. DMR-0306239), and by ORNL, managed by UT-Battelle, LLC, for the U.S. Department of Energy under Contract No. DE-AC05-00OR22725. The calculations were performed at ORNL's Center for Computational Sciences.

[1] P. Segovia, D. Purdie, M. Hengsberger, and Y. Baer, Nature (London) **402**, 504 (1999).
[2] R. Losio *et al.*, Phys. Rev. Lett. **86**, 4632 (2001).
[3] H. Ishil *et al.*, Nature (London) **426**, 540 (2003).
[4] F. J. Himpsel, J. E. Ortega, G. J. Mankey, and R. F. Willis, Adv. Phys. **47**, 511 (1998).
[5] J.-L. Lin *et al.*, Appl. Phys. Lett. **78**, 829 (2001).
[6] J. R. Ahn, H. W. Yeom, E. S. Cho, and C. Y. Park, Phys. Rev. B **69**, 233311 (2004).
[7] Z. Gai, G. A. Farnan, J. P. Pierce, and J. Shen, Appl. Phys. Lett. **81**, 742 (2002).
[8] J. Shen *et al.*, Phys. Rev. B **56**, 2340 (1997).
[9] V. Repain, J. M. Berroir, S. Rousset, and J. Lecoeur, Surf. Sci. **447**, L152 (2000).
[10] P. Gambardella, M. Blanc, L. Bürgi, K. Kuhnke, and K. Kern, Surf. Sci. **449**, 93 (2000).
[11] H. J. Elmers *et al.*, Phys. Rev. Lett. **73**, 898 (1994).
[12] J. Figuera *et al.*, Appl. Phys. Lett. **66**, 1006 (1995).
[13] D. Spišák and J. Hafner, Phys. Rev. B **65**, 235405 (2002).
[14] D. Spišák and J. Hafner, Phys. Rev. B **67**, 134434 (2003).
[15] M. Eisenbach, B. L. Györffy, G. M. Stocks, and B. Újfalussy, Phys. Rev. B **65**, 144424 (2002).
[16] G. Kresse and J. Hafner, Phys. Rev. B **47**, 558 (1993); G. Kresse and J. Furthmüller, *ibid.* **54**, 11169 (1996).
[17] J. P. Perdew and Y. Wang, Phys. Rev. B **45**, 13244 (1992).
[18] D. Vanderbilt, Phys. Rev. B **41**, 7892 (1990); G. Kresse and J. Hafner, J. Phys. Condens. Matter **6**, 8245 (1994).
[19] M. Methfessel and A. T. Paxton, Phys. Rev. B **40**, 3616 (1989).
[20] H. Jonsson, G. Mills, and K. W. Jacobsen, in *Classical and Quantum Dynamics in Condensed Phase Simulations*, edited by B. J. Berne, G. Ciccotti, and D. F. Coker (World Scientific, Singapore, 1998).
[21] D. C. Schlößer, L. K. Verheij, G. Rosenfeld, and G. Comsa, Phys. Rev. Lett. **82**, 3843 (1999).
[22] J. Shen (private communication).
[23] R. Stumpf and M. Scheffler, Phys. Rev. B **53**, 4958 (1996).
[24] Z. Zhang, X. Chen, and M. G. Lagally, Phys. Rev. Lett. **73**, 1829 (1994).
[25] P. E. Blöchl, Phys. Rev. B **50**, 17953 (1994); G. Kresse and D. Joubert, *ibid.* **59**, 1758 (1999).